



Original Article

Significance of Sex Differences on Gray Matter Atrophy in Alzheimer's Disease: A Voxel-Based Morphometry Study

Iman Beheshti¹, Hasan Demirel¹ and Chunlan Yang²

¹Biomedical image processing lab, Department of Electrical & Electronic Engineering, Eastern Mediterranean University, Gazimagusa, Mersin 10, Turkey

²College of Life Science and Bioengineering, Beijing University of Technology, Beijing, China

ARTICLE INFO

Received 13 Nov. 2015
Received in revised form 05 Dec. 2015
Accepted 15 Dec. 2015

Keywords:

Alzheimer's disease,
Sex,
Pattern of gray matter,
Voxel-based morphometry,
Statistical analysis.

Corresponding author: Biomedical image processing lab, Department of Electrical & Electronic Engineering, Eastern Mediterranean University, Gazimagusa, Mersin 10, Turkey

Tel.: +90 392 630-1301

E-mail address: iman.beheshti@cc.emu.edu.tr

ABSTRACT

Objective: Several voxel-based morphometry (VBM) studies have shown gray matter (GM) reduction as a result of Alzheimer's disease (AD). However, most of these have not considered GM atrophy in relation to sex differences.

Material and Methods: In this paper, we investigate global and local differences of GM using the VBM technique on 3-Tesla 3D T1-weighted magnetic resonance imaging (MRI), in four groups of people from the Alzheimer's Disease Neuroimaging Initiative (ADNI) database¹: males with AD (M-AD, n = 34), age-matched healthy male controls (M-HC, n= 34), females with AD (F-AD, n=34), and age-matched healthy female controls (F-HC, n= 34). The main scope of this research was to identify regions with significant GM loss in male and female cohorts. Analysis of variance (ANOVA) was used to compare means of GM differences between groups.

Results: The results indicate that sex plays a significant role in GM atrophy in people with AD. M-AD revealed significant GM reductions in the limbic lobe, the sub-lobar region, and parietal lobe, compared with M-HC, whereas in F-AD, significant GM reductions were located in the limbic lobe, the sub-lobar region, and several areas of the temporal lobe, compared with F-HC. The GM pattern differences between M-HC and F-HC, as well as between M-AD and F-AD, remained.

Conclusion: The statistical results obtained by VBM plus DARTEL showed that sex is an important factor in the pattern and severity of GM volume atrophy. The observed different pattern of GM volume reductions may help in understanding the root of AD mechanisms as biomarkers for detection and monitoring, and in explaining different behaviors in people with AD, based on sex.

Data used in this article were obtained from the Alzheimer's Disease Neuroimaging Initiative (ADNI) database (www.loni.ucla.edu/ADNI). ADNI investigators other than those listed above contributed to study design, implementation or data provision but did not participate in the analyses or writing of this report. The complete listing of ADNI investigators is available at http://www.loni.ucla.edu/ADNI/Data/ADNI_Authorship_List.pdf



Introduction

In older adults, Alzheimer's disease (AD) is the most common cause of dementia associated with whole brain volume loss, and the change in the region of the brain that is responsible for memory, learning, and higher executive functioning¹⁻⁵. It is estimated that 5.3 million American adults will suffer from AD in 2015, and this number is expected to increase to 16 million by 2050⁶. In the United States, of the estimated 5 million people over the age of 65 with the disease, 3.2 million are women⁶. Therefore, almost two thirds of people with AD in America are women^{6,7}. In addition to the fact that sex influences AD statistics, it also affects the character of the disease. Men affected with AD are more likely to show aggression, preoccupation with bodily functions, and apathy⁸. In contrast, women affected with AD show more reclusive behavior, emotional lability, hoarding, and refusal of help⁸. Therefore, different behaviors in people affected with AD differ between men and women. Previous studies have shown that males and females have different brain structures and functions. Sex differences in the brain, such as in brain anatomy, age-related decline in brain volume, and brain glucose metabolism, have been documented, and may be important in understanding the etiology of AD⁹⁻¹¹. In addition, males and females have different hormonal physiology, and sex-specific hormones are known to have effects on the brain. Differences or similarities between males and females in the onset and progression of dementia may help to better diagnose AD, which would help scientists and clinicians to develop relevant, targeted treatments. Sex differences research in AD aims to improve early diagnosis, ensure a better quality of life, and develop more effective treatments. Among the various neuroimaging techniques that are used to reveal markers for the diagnosis of AD, such as structural magnetic resonance imaging

(sMRI), functional magnetic resonance imaging (fMRI), positron emission tomography (PET), and single photon emission computed tomography (SPECT), sMRI is more widely used because of its noninvasiveness, and its excellent spatial resolution with good tissue contrast, and without radionuclides or radiation exposure, as is observed with PET or SPECT¹²⁻¹⁴. Voxel-based morphometry (VBM), introduced by Ashburner and Friston, has been developed to provide a powerful method of making group-wise comparisons between structural MRI scans showing disease versus normal controls^{15,16}. VBM can be used to assess whole brain structure with voxel-by-voxel comparisons, and has been developed to analyze tissue concentrations or volumes between participant groups to distinguish degenerative diseases from dementia^{13,15,17}. VBM has recently been applied to detect early atrophic changes in AD^{12,18-24}. To promote inter-subject registration of MRI images, we applied Diffeomorphic Anatomic Registration Through Exponentiated Lie algebra algorithm (DARTEL), which has been introduced to optimize the sensitivity of such analyses by using the Levenberg-Marquardt strategy, as compared to standard VBM²⁵⁻²⁷. Moreover, the DARTEL algorithm leads to the provision of precise, accurate localization of structural damage on the MRI images^{12,13}. Several recent studies have reported sex differences in gray matter (GM) in healthy individuals and healthy young^{11,28,29}. The current study used a cross-sectional analysis to examine differences in GM atrophy in AD by using the VBM technique plus the DARTEL approach. In this context, overall and regional structural GM alterations were investigated on a voxel-by-voxel basis using analysis of variance (ANOVA) among four groups of participants. The four groups included males with AD (M-AD, n = 34),



age-matched healthy male controls (M-HC, $n=34$), females with AD (F-AD, $n=34$), and age-matched healthy female controls (F-HC, $n=34$). The results obtained from 34 patients with AD were compared to 34 HC in each cohort. Females with AD showed more significant GM atrophy in the entire brain and in different areas, compared to males with AD. M-AD revealed significant GM reductions in the limbic lobe, the sub-lobar region, and parietal lobe, compared with M-HC, whereas in F-AD, significant GM reductions were located in the limbic lobe, the sub-lobar region, and several areas of the temporal lobe, compared with F-HC. According to the literature, age, family history, apolipoprotein E (APOE)- $\epsilon 4$ and genetics are the main factors in development of AD^{6,30,31}. In addition to these factors, using VBM analysis we show that sex is another dominant factor related to the distribution of GM atrophy in people with AD.

The remainder of this paper is arranged as follows: Section two gives statistics regarding the data used in this study; section three describes MRI processing and data analysis; section four presents the results of the statistical analysis performed on the MRI data; a discussion and suggestions for future research prospects are presented in section five; and section six is dedicated to conclusions.

Materials

MRI parameters

All MRI scans used in this study were obtained from the Alzheimer's Disease Neuroimaging Initiative (ADNI) database (www.loni.ucla.edu/ADNI) using 3 T scanners manufactured by Siemens. Acquisition parameters on the Siemens scanner are Acquisition Plane=Sagittal, Acquisition Type=3D, Coil=PA, Field Strength=3.0 tesla, Flip Angle=9.0 degree, Matrix X=240.0 pixels, Matrix Y=256.0

pixels, Matrix Z=176, Mfg Model=Skyra, Pixel Spacing X=1.0 mm, Pixel Spacing Y=1.0 mm, Pulse Sequence=GR/IR, Slice Thickness=1.2 mm, TE=2.98 ms, TI=900 ms, TR=2300 ms, and Weighting=T1. The scan protocols were identical for all MRIs.

Participant Characteristics

All participants initially underwent several neuropsychological examinations, resulting in several clinical characteristic indicators, including Mini Mental State Examination (MMSE) score and Clinical Dementia Ratio (CDR) score. On the basis of the aforementioned criteria (2.1 MRI parameters), 200 samples were randomly obtained from the ADNI database. A quota sampling technique was then used to select 136 samples, which were matched on the basis of age and clinical characteristics (e.g. MMSE and CDR) and arranged in four groups (Table 1). The first cohort contained females that were divided into groups of healthy individuals and those with AD. The F-HC group contained 34 participants with ages ranging from 66 to 84 years, MMSE score ranging from 28 to 30, and a CDR score of zero. A total of 34 females with AD were selected for the F-AD group, and their ages ranged from 61 to 89 years, while their MMSE and CDR scores ranged from 16 to 25 and 0.5 to 2, respectively. The second cohort contained males that were divided into groups of healthy individuals and those with AD. The M-HC group comprised 34 individuals with ages ranging from 60 to 82 years, while MMSE score ranged from 28 to 30, and CDR score was zero. A total of 34 males with AD were selected for the M-AD group, and their ages ranged from 62 to 88 years, while their MMSE score ranged from 15 to 25, and their CDR score ranged from 0.5 to 2 (see Table 1). In a direct comparison of the four groups, ANOVA showed no significant difference in age ($F(3,135) = 0.08$, $p = NS$). There were no

significant differences in MMSE score ($p = \text{NS}$) and CDR score ($p = \text{NS}$) between F-AD versus M-AD and F-HC versus M-HC, respectively.

Methods

In this section, we describe the computational processes applied to the data. The VBM process is summarized, and details are provided with regard to its application to AD.

Detection of gray matter pattern in AD: VBM analysis

Data preprocessing was performed using Statistical Parameter Mapping software version 8 (<http://www.fil.ion.ucl.ac.uk/spm>), and the VBM toolbox (<http://dbm.neuro.uni-jena.de/vbm>) with default settings. The VBM8-toolbox uses the unified segmentation model, in which structural MRIs are bias-corrected, segmented into white matter (WM), gray matter (GM), and cerebrospinal fluid (CSF) components, and registered within the same model^{32,33}. The VBM technique has several advantages compared to volumetric approaches, such as allowing for investigation of structural differences in areas with poorly defined structural landmarks (e.g., prefrontal areas) and explorative analysis of structural differences³³. Registration to standard MNI-space (<http://www.mni.mcgill.ca/>) consists of a linear affine transformation and a nonlinear deformation using high-dimensional DARTEL normalization²⁶. This procedure uses the DARTEL template of 550 healthy control participants (defined by default settings VBM8)^{21,33}. In the present study, the normalized segmented images were modulated by applying a nonlinear deformation. This allows the comparison of absolute amounts of tissue corrected for individual differences in brain size. Finally, the segmented images were spatially

smoothed with an 8 mm Full-Width-Half-Maximum (FWHM) Gaussian kernel. Total GM volume (GMV), WM volume (WMV), and CSF volume were obtained from the VBM8 toolbox, on the basis of segmented images, and total intracranial volume (TIV) was calculated as the sum of GMV, WMV, and CSF volume. After spatial preprocessing, the smoothed, modulated, DARTEL-warped and normalized gray matter datasets were used for statistical analysis. Regional GM volume changes were generated by voxel-based analysis over the entire brain.

Statistical analysis

Morphological group differences for normalized, segmented, smoothed, DARTEL-warped, and modulated GM images among four groups were analyzed using analysis of variance (ANOVA) in SPM8. Age and TIV were applied into the matrix design as nuisance variables. An absolute threshold for masking of around 0.1 was used to avoid possible edge effects between GM and WM or CSF. Group comparisons were assessed by using Family-Wise Error (FWE) at a threshold of $p < 0.05$, corrected for multiple comparisons, and statistical significance was determined using an extent threshold of 100. Between-group differences in demographics and clinical parameters among or between groups were examined using Statistical Package for Social Sciences software (SPSS version 16.0, <http://www.spss.com/>). The normalized GMV between groups was compared using ANOVA followed by a Tukey multiple comparison test, and $p < 0.05$ was considered significant.

Results

Global changes in volume of GM based on sex

TIV and GM are expressed as mean and standard deviation (SD) in volume (ml),

and Figure 1a shows GMV (ml) for all groups. In order to correct for variation in head size, the GMVs of all the participants were normalized by dividing the individual value by the TIV of the respective participants (see figure 1b). The ANOVA showed significant differences between normalized GM (GM/TIV) in the four groups ($F(3,135) = 18.96, p < 0.001$). In the M-HC and M-AD groups, the normalized GM was 0.41 ± 0.02 and 0.39 ± 0.02 ($MD = 0.02, p < 0.05$), respectively, and in the F-HC and F-AD groups, the normalized GM was 0.43 ± 0.01 and 0.40 ± 0.02 , respectively ($MD = 0.032, p < 0.001$). A summary of the statistical analyses is presented in Tables 2 and 3, and in Figure 1. When we compared normalized GM in the male cohort versus the female cohort, it was clear that global normalized GM atrophy in whole brain in females was significantly more than in males ($MD = 0.03$ in females and $MD = 0.02$ in males).

VBM of GM analysis

VBM comparisons of GM in M-AD versus M-HC

In the male cohort, VBM plus DARTEL revealed a significant decline of GM volume in the right parahippocampal gyrus, left lentiform nucleus, and right supramarginal gyrus (see Table 4 and Figure 2a for more details). Figure 3.a illustrates six three-dimensional voxel clusters of group comparison representing relative gray matter atrophy in patients with AD compared to healthy controls in male cohort.

VBM comparisons of GM in F-AD group versus F-HC group

The highest level of reductions of GM volume of the F-AD group compared to the F-HC group were located in the right parahippocampal gyrus, left lentiform nucleus, left middle temporal gyrus, and left

middle temporal gyrus, respectively (see Table 4 and Figure 2.b). Figure 3.b illustrates six three-dimensional voxel clusters of group comparison representing relative gray matter atrophy in patients with AD compared to healthy controls in female cohort.

VBM comparisons of GM in M-AD versus F-AD and M-HC versus F-HC

ANOVA showed the decline of GM volume in M-AD compared to F-AD in the left inferior semi-lunar lobule, the left lentiform nucleus, and the left insula (see Table 4 and Figure 2c for more details). In addition, the most significant differences in GM volume in the M-HC compared to the F-HC were located in the right superior frontal gyrus, left inferior semi-lunar lobule, right postcentral gyrus, and left precuneus, respectively (see Table 4, Figure 2.d). Six three-dimensional voxel clusters of group comparison representing relative gray matter changes in M-AD compared to F-AD and M-HC compared to F-HC are shown in Figure 3.c and Figure 3.d, respectively. The reverse contrast showed no significant differences in GM volume change in F-AD compared with M-AD, and F-HC compared with M-HC, respectively.

Discussion

In this study, we examined sex differences in GM pattern changes in people with AD compared to healthy controls. VBM plus DARTEL study of structural MRI indicated different GM patterns in a number of specific regions and severity of GM atrophy in the males and females with AD, compared to the healthy controls. The results revealed that global GM reduction in the female cohort (F-AD versus F-HC) was around 1.4 times greater than GM reduction in the male cohort (M-AD versus M-HC). These results correspond to a 4.8% reduction in GM in the male cohort

compared to a 6.9% reduction in the female cohort. Several significant explanations may underlie our results. The first explanation is due to structural differences. Males normally have a larger head size and cerebral brain volume than females (~ 10 %) ³⁴, so one would anticipate that males are capable of enduring more pathology, and have significantly reduced AD severity at the same level of pathology ³⁵. The second explanation is due to functional differences. Some recent studies have shown that males have more pronounced cerebral metabolic deficits compared to females at the same level of cognitive impairment. Thus, it can be suggested that the greater brain reserve in males may aid them in enduring more pathology than females ³⁶⁻³⁸. The final explanation is down to genetic differences. The $\epsilon 4$ allele of the APOE gene has a higher tortuous effect on hippocampal pathology, cortical thickness, and memory performance in females with AD compared to males with the disease ^{39,40}. In addition, the Met66 allele of the brain-derived neurotrophic factor gene is correlated with an increased risk of AD in females, but not in males ⁴¹. In particular, we observed that GM volume reduction in the male cohort was confined to the parahippocampal gyrus, lentiform nucleus, and supramarginal gyrus, whereas the female cohort showed GM atrophy in several regions, although it was primarily located in the parahippocampal gyrus, lentiform nucleus, and several parts of the middle temporal gyrus. Our results showed that there were no significant differences in GM volume for the male cohort in the middle temporal gyrus, thalamus, and caudate head, which is given in ⁴². The highest GM reduction in both cohorts was observed in the area contributing to memory decline and other cognitive functions. This finding is similar to ^{42,43}, but the female cohort showed a greater peak Z-score of GM reduction. In contrast to the male cohort,

there appeared to be more numerous and more extensive GM abnormalities in the female cohort, which indicates that the progressive GM atrophy is sex-associated. We also noted that those in the female AD cohort compared to the F-HC showed a reduced volume in the areas involved in emotion. This might be the main reason why females with AD show more reclusive behavior, emotional lability, hoarding, and refusal of help. ANOVA showed there were no significant differences of GM volume deficit in F-AD compared to M-AD and in F-HC compared to M-HC, respectively. The reason for this may be that, due to sex chromosomes and hormones, females typically have a higher percentage of GM in several brain regions compared to males ^{37,44}. In a direct comparison between M-AD and F-AD, ANOVA showed some GM changes in the posterior lobe and sub-lobar region. In addition, ANOVA showed a GM deficit in the frontal lobe, posterior lobe, parietal lobe, and occipital lobe in M-HC compared to F-HC. This finding concurs with those of many previous studies, which reported that the GM ratio was consistently higher in the frontal, parietal, temporal, and occipital lobes in females versus males ⁴⁴⁻⁴⁶. A reasonable assessment of our finding is that although global GM decreases linearly with age in healthy adults, male and female, this decrease is steeper in males ^{10,44}. The reasons for these differences are not clear, but may be related to female sex steroids. As part of future studies on GM atrophy in patients with AD exploiting gender differences, we suggest considering the effect of duration of education, socioeconomic status, risk behavior, social and work-related stressors, and lifestyle ³⁷. Another priority for future studies will be to use other registration methods, such as LDDMM ⁴⁷. These methods could be further used to evaluate the accuracy of inter-

subject registration in GM volume changes in patients with AD.

Conclusion

In conclusion, we used a statistical analysis by VBM plus DARTEL to examine global and regional GM atrophy patterns in people with AD, according to sex. The results have considerable implications for the development of therapies for those with this disease. The findings indicate that AD causes different patterns of GM atrophy and morphological changes in males and females. The atrophy volume is less in males, compared to females. Females with AD show more widespread GM atrophic changes in the different regions. Therefore, we suggest to seclude patients with AD based on the sex for future research. It is worth noting that knowing the difference between the male and female patterns of GM atrophy may be significant in helping researchers better decipher an individual's response to drug therapy.

Compliance with ethical standards

Funding

There was no financial support for this work.

Conflict of Interest

All authors have indicated no financial conflicts of interest.

Ethical approval

All authors confirm that our research involving human participants which data used in this article were obtained from the Alzheimer's Disease Neuroimaging Initiative (ADNI) database (www.loni.ucla.edu/ADNI).

Informed consent

Informed consent was obtained from all individual participants included in the study.

Disclosure statement

This was not an industry supported study. The authors have indicated no financial conflicts of interest.

References

1. Carter CL, Resnick EM, Mallampalli M, Kalbarczyk A. Sex and Gender Differences in Alzheimer's Disease: Recommendations for Future Research. *J Women's Heal.* 2012;21(10):1018-1023. doi:10.1089/jwh.2012.3789.
2. Prokšelj T, Jerin A, Muck-Seler D, Kogoj A. Decreased platelet serotonin concentration in Alzheimer's disease with involuntary emotional expression disorder. *Neurosci Lett.* 2014;578:71-74. doi:10.1016/j.neulet.2014.06.034.
3. Luo J, Li S, Qin X, *et al.* Meta-analysis of the association between CR1 polymorphisms and risk of late-onset alzheimer's disease. *Neurosci Lett.* 2014;578:165-170. doi:10.1016/j.neulet.2014.06.055.
4. Ben Ahmed O, Mizotin M, Benois-Pineau J, Allard M, Catheline G, Ben Amar C. Alzheimer's disease diagnosis on structural MR images using circular harmonic functions descriptors on hippocampus and posterior cingulate cortex. *Comput Med Imaging Graph.* 2015;44:13-25. doi:10.1016/j.compmedimag.2015.04.007.
5. Zhang Y, Wang S, Phillips P, Dong Z, Ji G. Biomedical Signal Processing and Control Detection of Alzheimer 's disease and mild cognitive impairment based on structural volumetric MR images using 3D-DWT and WTA-KSVM trained by PSOTVAC. *Biomed Signal Process Control.* 2015;21:58-73. doi:10.1016/j.bspc.2015.05.014.
6. Alzheimer's Association | Alzheimer's Disease and Dementia. 2015. <http://www.alz.org/>. Accessed April 5, 2015.
7. Hebert LE, Weuve J, Scherr P a., Evans D a. Alzheimer disease in the United States

- (2010-2050) estimated using the 2010 census. *Neurology*. 2013;80(19):1778-1783. doi:10.1212/WNL.0b013e31828726f5.
8. Ott BR, Tate CA, Gordon NM, Heindel WC. Gender differences in the behavioral manifestations of Alzheimer's disease. *J Am Geriatr Soc*. 1996;44(5):583-587.
 9. Cheng Y, Chou KH, Decety J, *et al*. Sex differences in the neuroanatomy of human mirror-neuron system: A voxel-based morphometric investigation. *Neuroscience*. 2009;158(2):713-720. doi:10.1016/j.neuroscience.2008.10.026.
 10. Good CD, Johnsrude I, Ashburner J, Henson RN, Friston KJ, Frackowiak RS. Cerebral asymmetry and the effects of sex and handedness on brain structure: a voxel-based morphometric analysis of 465 normal adult human brains. *Neuroimage*. 2001;14(3):685-700. doi:10.1006/nimg.2001.0857.
 11. Gur RC, Turetsky BI, Matsui M, *et al*. Sex differences in brain gray and white matter in healthy young adults: correlations with cognitive performance. *J Neurosci*. 1999;19(10):4065-4072.
 12. Matsuda H, Mizumura S, Nemoto K, *et al*. Automatic voxel-based morphometry of structural MRI by SPM8 plus diffeomorphic anatomic registration through exponentiated Lie algebra improves the diagnosis of probable Alzheimer disease. *Am J Neuroradiol*. 2012;33(6):1109-1114. doi:10.3174/ajnr.A2935.
 13. Nakatsuka T, Imabayashi E, Matsuda H, Sakakibara R, Inaoka T, Terada H. Discrimination of dementia with Lewy bodies from Alzheimer's disease using voxel-based morphometry of white matter by statistical parametric mapping 8 plus diffeomorphic anatomic registration through exponentiated Lie algebra. *Neuroradiology*. 2013;55(5):559-566. doi:10.1007/s00234-013-1138-9.
 14. Beg MF, Raamana PR, Barbieri S, Wang L. Comparison of four shape features for detecting hippocampal shape changes in early Alzheimer's. *Stat Methods Med Res*. 2012. doi:10.1177/0962280212448975.
 15. Ashburner J, Friston KJ. Voxel-based morphometry--the methods. *Neuroimage*. 2000;11(6 Pt 1):805-821. doi:10.1006/nimg.2000.0582.
 16. Comley R a., Cervenka S, Palhagen SE, *et al*. A comparison of gray matter density in restless legs syndrome patients and matched controls using voxel-based morphometry. 2012;i:28-32. doi:10.1111/j.1552-6569.2010.00536.x.
 17. Vemuri P, Jack CR. Role of structural MRI in Alzheimer's disease. *Alzheimers Res Ther*. 2010;2(4):23. doi:10.1186/alzrt47.
 18. Hirata Y, Matsuda H, Nemoto K, *et al*. Voxel-based morphometry to discriminate early Alzheimer's disease from controls. *Neurosci Lett*. 2005;382(3):269-274. doi:10.1016/j.neulet.2005.03.038.
 19. Karas GB, Burton EJ, Rombouts S a RB, *et al*. A comprehensive study of gray matter loss in patients with Alzheimer's disease using optimized voxel-based morphometry. *Neuroimage*. 2003;18(4):895-907. doi:10.1016/S1053-8119(03)00041-7.
 20. Son JH, Han DH, Min KJ, Kee BS. Correlation between gray matter volume in the temporal lobe and depressive symptoms in patients with Alzheimer's disease. *Neurosci Lett*. 2013;548:15-20. doi:10.1016/j.neulet.2013.05.021.
 21. Beheshti I, Demirel H. Probability distribution function-based classification of structural MRI for the detection of Alzheimer's disease. *Comput Biol Med*. 2015;64:208-216. doi:10.1016/j.combiomed.2015.07.006.
 22. Beheshti I, Demirel H. Feature-ranking-based Alzheimer's disease classification from structural MRI. *Magn Reson Imaging*. 2015. doi:10.1016/j.mri.2015.11.009.
 23. Bron EE, Smits M, van der Flier WM, *et al*. Standardized evaluation of algorithms for computer-aided diagnosis of dementia based on structural MRI: The CADDementia challenge. *Neuroimage*. 2015;111:562-579. doi:10.1016/j.neuroimage.2015.01.048.
 24. Moradi E, Pepe A, Gaser C, Huttunen H, Tohka J. Machine learning framework for early MRI-based Alzheimer's conversion prediction in MCI subjects. *Neuroimage*. 2015;104:398-412. doi:10.1016/j.neuroimage.2014.10.002.

25. Modi S, Bhattacharya M, Singh N, Tripathi RP, Khushu S. Effect of visual experience on structural organization of the human brain: A voxel based morphometric study using DARTEL. *Eur J Radiol.* 2012;81(10):2811-2819. doi:10.1016/j.ejrad.2011.10.022.
26. Ashburner J. A fast diffeomorphic image registration algorithm. *Neuroimage.* 2007;38(1):95-113. doi:10.1016/j.neuroimage.2007.07.007.
27. Klein A, Andersson J, Ardekani B a., *et al.* Evaluation of 14 nonlinear deformation algorithms applied to human brain MRI registration. *Neuroimage.* 2009;46(3):786-802. doi:10.1016/j.neuroimage.2008.12.037.
28. Luders E, Gaser C, Narr KL, Toga AW. Why sex matters: brain size independent differences in gray matter distributions between men and women. *J Neurosci.* 2009;29(45):14265-14270. doi:10.1523/JNEUROSCI.2261-09.2009.
29. Chen X, Sachdev PS, Wen W, Anstey KJ. Sex differences in regional gray matter in healthy individuals aged 44-48 years: a voxel-based morphometric study. *Neuroimage.* 2007;36(3):691-699. doi:10.1016/j.neuroimage.2007.03.063.
30. Terry Jr a. V, Buccafusco JJ. The Cholinergic Hypothesis of Age and Alzheimer's Disease- Related Cognitive Deficits: Recent Challenges and Their Implications for Novel Drug Development. *J Pharmacol Exp Ther.* 2003;306(3):821-827. doi:10.1124/jpet.102.041616.For.
31. Lindsay J, Laurin D, Verreault R, *et al.* Risk factors for Alzheimer's disease: A prospective analysis from the Canadian Study of Health and Aging. *Am J Epidemiol.* 2002;156(5):445-453. doi:10.1093/aje/kwf074.
32. Ashburner J, Friston KJ. Unified segmentation. *Neuroimage.* 2005;26(3):839-851. doi:10.1016/j.neuroimage.2005.02.018.
33. Cousijn J, Wiers RW, Ridderinkhof KR, Van den Brink W, Veltman DJ, Goudriaan AE. Grey matter alterations associated with cannabis use: Results of a VBM study in heavy cannabis users and healthy controls. *Neuroimage.* 2012;59(4):3845-3851. doi:10.1016/j.neuroimage.2011.09.046.
34. Giedd JN, Raznahan A, Mills KL, Lenroot RK. Review: magnetic resonance imaging of male/female differences in human adolescent brain anatomy. *Biol Sex Differ.* 2012;3(1):19. doi:10.1186/2042-6410-3-19.
35. Barnes, Lisa L., Robert S. Wilson, Julia L. Bienias, Julie A. Schneider, Denis A. Evans and DAB. Sex differences in the clinical manifestations of Alzheimer disease pathology. *Arch Gen Psychiatry.* 2005;62(6):685-691.
36. Pernecky R, Drzezga a., Diehl-Schmid J, Li Y, Kurz a. Gender differences in brain reserve: An 18F-FDG PET study in Alzheimer's disease. *J Neurol.* 2007;254(10):1395-1400. doi:10.1007/s00415-007-0558-z.
37. Mielke MM, Vemuri P, Rocca W a. Clinical epidemiology of Alzheimer's disease: Assessing sex and gender differences. *Clin Epidemiol.* 2014;6(1):37-48. doi:10.2147/CLEP.S37929.
38. Pernecky, R. Diehl-Schmid, Janine. Forstl, Hans. Drzezga, Alexander. Kurz A. Male gender is associated with greater cerebral hypometabolism in frontotemporal dementia: evidence for sex-related cognitive reserve. *Int J Geriatr Psychiatry.* 2007;22:1135-1140. doi:10.1002/gps.1803.
39. Liu, Yawu, Teemu Paajanen, Eric Westman, Lars-Olof Wahlund, Andrew Simmons, Catherine Tunnard TS *et al.* Effect of APOE ε4 allele on cortical thicknesses and volumes: the AddNeuroMed study. *J Alzheimer's Dis.* 2010;21(3):947-966. doi:10.3233/JAD-2010-100201.
40. Damoiseaux JS, Seeley WW, Zhou J, *et al.* Gender Modulates the APOE e 4 Effect in Healthy Older Adults : Convergent Evidence from Functional Brain Connectivity and Spinal Fluid Tau Levels. 2012;32(24):8254-8262. doi:10.1523/JNEUROSCI.0305-12.2012.
41. Fukumoto N, Fujii T, Combarros O, *et al.* Sexually dimorphic effect of the Val66Met polymorphism of BDNF on susceptibility to Alzheimer's disease: New data and meta-analysis. *Am J Med Genet Part B Neuropsychiatr Genet.* 2010;153(1):235-242. doi:10.1002/ajmg.b.30986.

42. Guo X, Wang Z, Li K, *et al*. Voxel-based assessment of gray and white matter volumes in Alzheimer's disease. *Neurosci Lett*. 2010;468(2):146-150.
doi:10.1016/j.neulet.2009.10.086.
43. Stoub TR, deToledo-Morrell L, Stebbins GT, Leurgans S, Bennett D a, Shah RC. Hippocampal disconnection contributes to memory dysfunction in individuals at risk for Alzheimer's disease. *Proc Natl Acad Sci U S A*. 2006;103(26):10041-10045.
doi:10.1073/pnas.0603414103.
44. Cosgrove KP, Mazure CM, Staley JK. Evolving knowledge of sex differences in brain structure, function, and chemistry. *Biol Psychiatry*. 2007;62(8):847-855.
doi:10.1016/j.biopsych.2007.03.001.Evolving
45. Haier RJ, Jung RE, Yeo R a., Head K, Alkire MT. The neuroanatomy of general intelligence: Sex matters. *Neuroimage*. 2005;25(1):320-327.
doi:10.1016/j.neuroimage.2004.11.019.
46. Allen JS, Damasio H, Grabowski TJ, Bruss J, Zhang W. Sexual dimorphism and asymmetries in the gray-white composition of the human cerebrum. *Neuroimage*. 2003;18(4):880-894.
doi:10.1016/S1053-8119(03)00034-X.
47. Miller MI, Beg MF, Ceritoglu C, Stark C. Increasing the power of functional maps of the medial temporal lobe by using large deformation diffeomorphic metric mapping. *Proc Natl Acad Sci U S A*. 2005;102(27):9685-9690.
doi:10.1073/pnas.0503892102.

Table 1. Characteristics of patients with Alzheimer's disease are compared with healthy controls according to sex

	F-AD	F-HC	M-AD	M-HC
Age	74.01±7.09	74.03±4.79	74.64±5.71	74.25±5.18
Number	34	34	34	34
MMSE	22.73±2.43	29.38±0.69	22.73±2.72	29.38±0.73
CDR	0.75±0.39	0.0±0	0.75±0.39	0.0±0

Note: All data are presented in mean ± standard deviation mode. AD, people with Alzheimer's disease; CDR, Clinical Dementia Rating; HC, healthy control participants; MMSE, Mini-Mental State Examination; F, Female; M, Male.

Table 2. Global volume measurement in the four groups

	F-AD	F-HC	M-AD	M-HC
TIV(ml)	1303±99	1286±87	1499±123	1473±125
GM (ml)	524±42	558±41	591±71	610±50
n-GM	0.40±0.02	0.43±0.01	0.39±0.02	0.41±0.02

Note: All data are presented in mean ± standard deviation mode; F, Female; M, Male; AD, people with Alzheimer's disease; HC, healthy control participants; TIV, total intracranial volume; GM, gray matter; n-GM, normalized gray matter (global GM/TIV).

Table 3. Comparative mean of normalized gray matter in the four groups

Variable	F-AD	F-HC	M-AD	M-HC
n-GM	MD	MD	MD	MD
F-AD	---	-0.032**	0.008	-0.012
F-HC	0.032**	---	0.040**	0.019*
M-AD	-0.008	-0.040**	---	-0.020*
M-HC	0.012	-0.019*	0.020*	----
F^{\dagger}	18.96*			

Note: F, Female; M, Male; AD, people with Alzheimer's disease; HC, healthy control participants; n-GM, normalized gray matter (global GM/TIV); MD, mean difference; F^{\dagger} , F test; * $p < 0.05$; ** $p < 0.001$.

Table 4. Regions of decreased gray matter volume in four groups

	Location of peak voxels	Hemisphere	Cluster level P (corrected)	Cluster size (no of voxels)	Talairach coordinates (x,y,z)	Z value (peak voxel)
Male HC > Male AD	Parahippocampal Gyrus	R	0.000	1165	26 -10 -14	6.24
	Lentiform Nucleus	L	0.000	1297	-25 -14 -8	6.16
	Supramarginal Gyrus	R	0.000	345	58 -44 27	5.6
Female HC > Female AD	Parahippocampal Gyrus	R	0.000	8415	32 -9 -16	7.13
	Lentiform Nucleus	L	0.000	4354	-25 -15 -8	6.72
	Middle Temporal Gyrus	L	0.000	246	-37 -1 -30	5.82
	Middle Temporal Gyrus	L	0.001	117	-53 -3 -12	5.44
	Middle Temporal Gyrus	L	0.002	481	-55 -45 3	5.22
	Middle Temporal Gyrus	L	0.005	158	-46 -63 -2	5.08
Female HC > Male HC	Superior Frontal Gyrus	R	0.000	583	4 53 -22	6.12
	Inferior Semi-Lunar Lobule	L	0.000	1102	-13 -75 -46	6.06
	Postcentral Gyrus	R	0.000	672	28 -32 59	5.86
	Precuneus	L	0.000	551	-24 -75 35	5.59
	Precentral Gyrus	R	0.001	428	-55 -8 34	5.46
	Precuneus	L	0.001	823	-1 -69 27	5.39
	Middle Occipital Gyrus	L	0.002	450	-49 -69 8	5.31
	Superior Temporal Gyrus	L	0.007	246	-52 -59 25	5.00
Female AD > Male AD	Inferior Parietal Lobule	L	0.009	210	-48 -61 48	4.92
	Inferior Semi-Lunar Lobule	L	0.003	440	-14 -72 -46	5.20
	Lentiform Nucleus	L	0.003	460	-19 17 3	5.18
	Insula	L	0.003	358	-42 -29 20	5.17

Note: Anatomical regions were derived from the Talairach Client program; L, left hemisphere; R, right hemisphere; MNI, Montreal Neurological Institute; (FDR-corrected at $p < 0.05$).

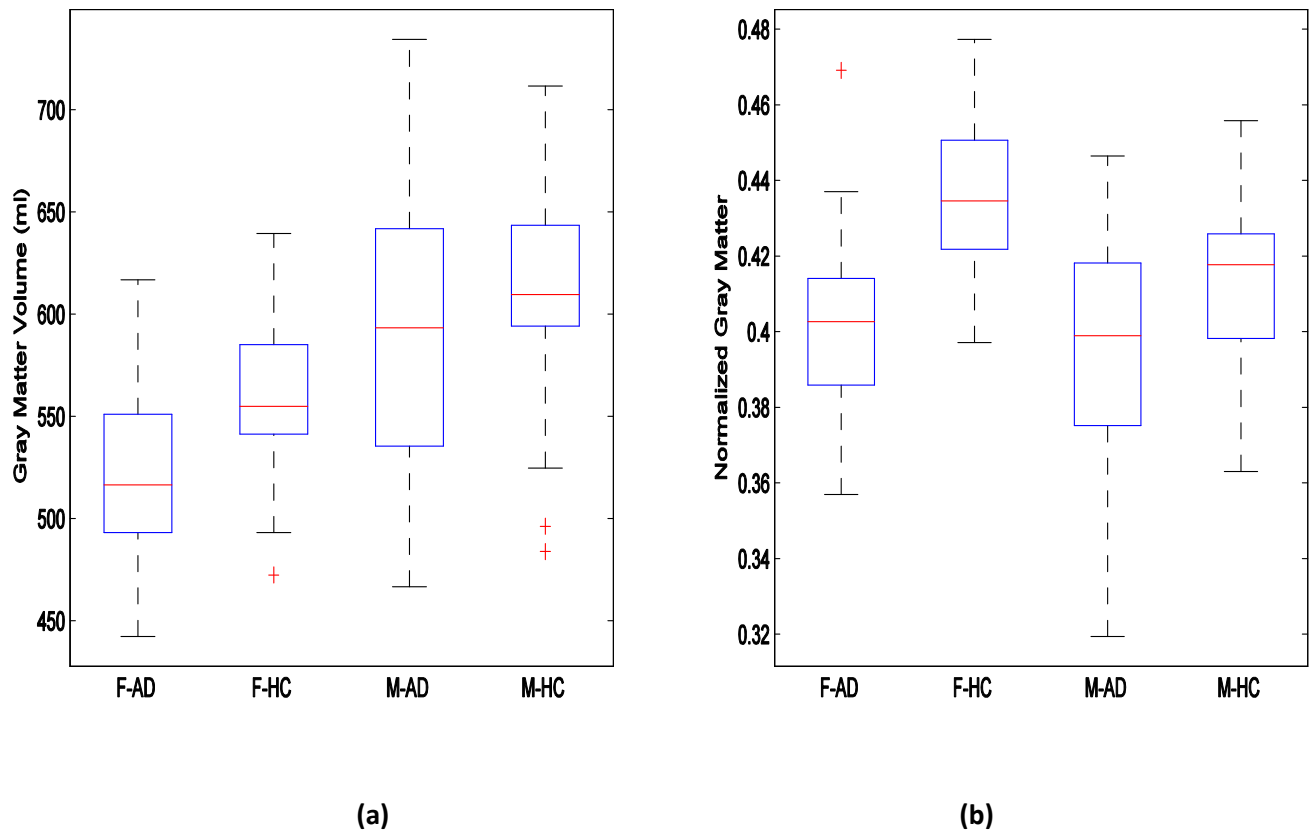


Fig. 1: Gray matter and normalized gray matter (a and b, respectively) for the four groups. AD, people with Alzheimer's disease; HC, healthy control participants; GM= gray matter; nGM (normalized gray matter) = gray matter volume over total intracranial volume (TIV).

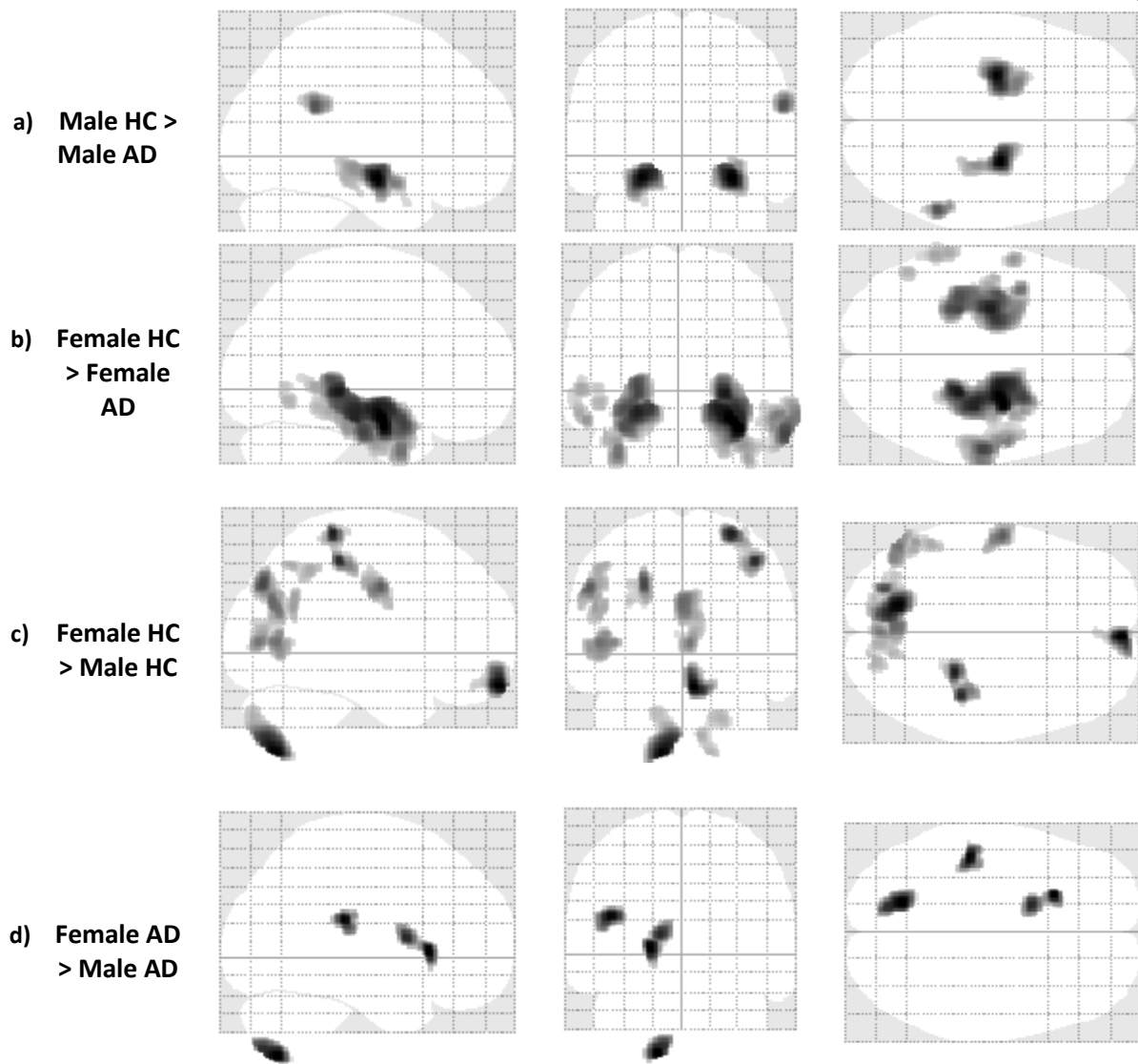


Fig. 2: Comparison of gray matter volume changes in the four groups by VBM using SPM8 plus DARTEL (FWE corrected at $p < 0.05$ and extend threshold $K = 100$).

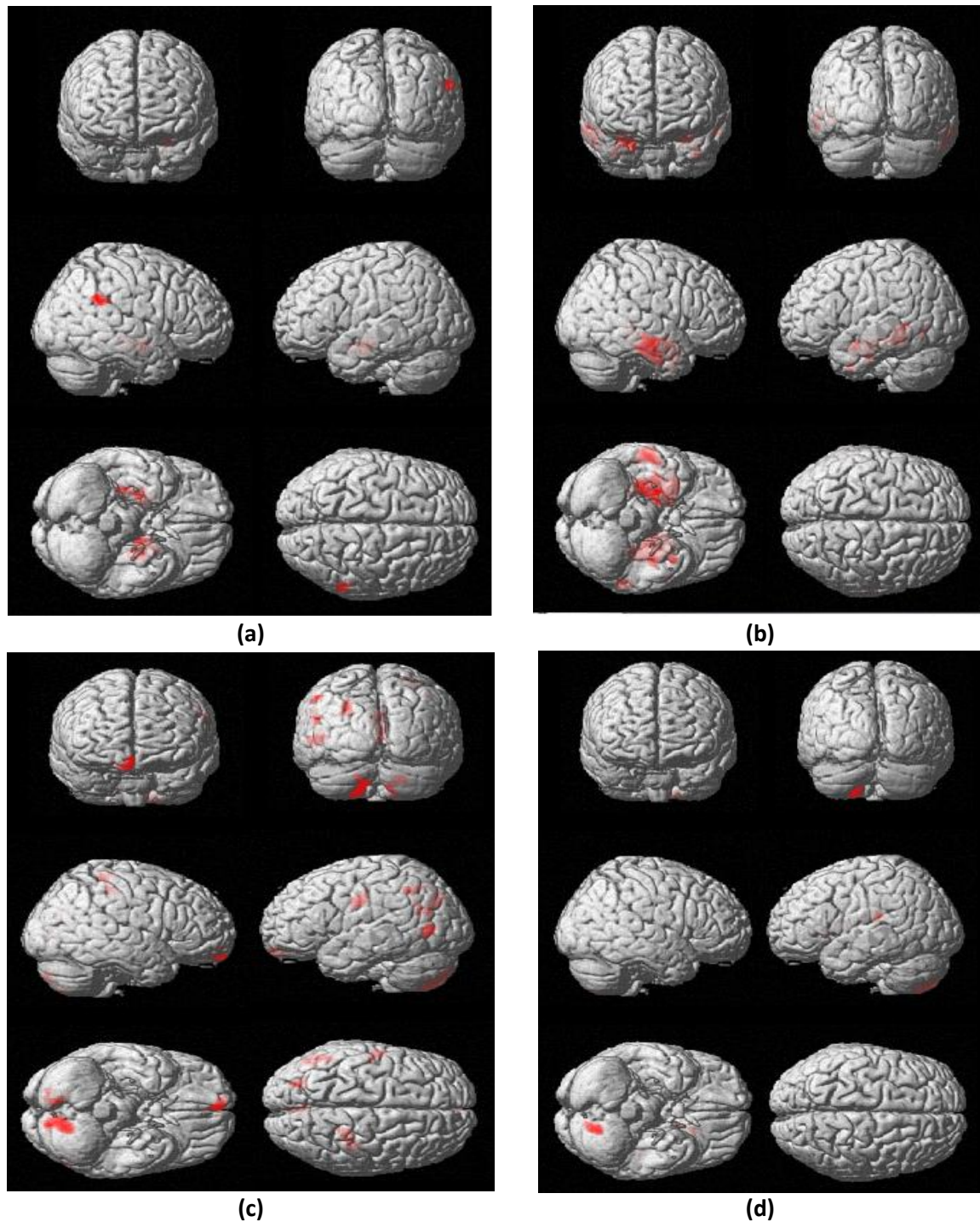


Fig. 3: Three-dimensional reconstruction of the brain showing gray matter changes in four groups using VBM technique plus DARTEL. The regions of gray matter loss are shown from anterior, posterior, right lateral, left lateral, inferior and superior view, respectively. The red region represents the region of gray matter loss. (a) Male HC > Male AD, (b) Female HC > Female AD, (c) Female HC > Male HC and (d) Female AD > Male AD.